Report

Current Biology

Bias in Human Path Integration Is Predicted by Properties of Grid Cells

Highlights

- Deforming the shape of a familiar room causes errors in human path integration
- These errors are predicted by properties of grid cells
- These findings explicate the way grid cells may function in human path integration

Authors

Xiaoli Chen, Qiliang He, Jonathan W. Kelly, Ila R. Fiete, Timothy P. McNamara

Correspondence

t.mcnamara@vanderbilt.edu

In Brief

Path integration may depend on grid cells, which are found in the brains of several mammals and may provide an internal odometer. Based on findings from rat, Chen et al. predicted errors in human navigation in response to changes to a familiar room's shape. These predictions were confirmed in behavioral experiments using immersive virtual reality.

Chen et al., 2015, Current Biology *25*, 1771–1776
June 29, 2015
http://dx.doi.org/10.1016/j.cub.2015.05.031

CellPress

Current Biology
Report

Bias in Human Path Integration Is Predicted by Properties of Grid Cells

Xiaoli Chen,[1] Qiliang He,[1] Jonathan W. Kelly,[2] Ila R. Fiete,[3] and Timothy P. McNamara[1,*]
[1]Department of Psychology, Vanderbilt University, Nashville, TN 37240, USA
[2]Department of Psychology, Iowa State University, Ames, IA 50011, USA
[3]Center for Learning and Memory, The University of Texas, Austin, TX 78712, USA
*Correspondence: t.mcnamara@vanderbilt.edu
http://dx.doi.org/10.1016/j.cub.2015.05.031

SUMMARY

Accurate wayfinding is essential to the survival of many animal species and requires the ability to maintain spatial orientation during locomotion. One of the ways that humans and other animals stay spatially oriented is through path integration, which operates by integrating self-motion cues over time, providing information about total displacement from a starting point [1, 2]. The neural substrate of path integration in mammals may exist in grid cells, which are found in dorsomedial entorhinal cortex and presubiculum and parasubiculum in rats [3, 4]. Grid cells have also been found in mice, bats, and monkeys [5–7], and signatures of grid cell activity have been observed in humans [8, 9]. We demonstrate that distance estimation by humans during path integration is sensitive to geometric deformations of a familiar environment and show that patterns of path integration error are predicted qualitatively by a model in which locations in the environment are represented in the brain as phases of arrays of grid cells with unique periods and decoded by the inverse mapping from phases to locations. The periods of these grid networks are assumed to expand and contract in response to expansions and contractions of a familiar environment [10]. Biases in distance estimation occur when the periods of the encoding and decoding grids differ. Our findings explicate the way in which grid cells could function in human path integration.

RESULTS

Grid cells have multi-peaked receptive fields, with peaks occurring on every vertex of a triangular grid that spans the environment [4]. In rodents, when a familiar environment expands or contracts, the grid cell responses in the deformed environment parametrically expand or contract in the same direction, for at least a few hours, until the grid periods gradually return to their original values in the deformed space [10]. A key feature of the grid cell code is that it represents location as a set of spatial phases, relative to the periodic spatial activity patterns of different sets of grid cells with distinct spatial periods [11]. When a dimension of a familiar environment shrinks, the spatial periods of grid cells contract. As a result, the amount of phase increment for a fixed displacement between two locations will be greater for the contracted grid response than for the original grid from the familiar environment (Figure 1 and Supplemental Information). An ideal decoder of location from grid cell phases, constructed for the original grid periods but using input phases from the contracted grid, would estimate a larger than actual displacement between the two locations. We conjectured that these conditions might exist for humans if the outbound journey took place in the recently deformed environment but the return journey took place without vision, and therefore presumably with restored grid periods [12]. Under such conditions, the participant should overshoot the target according to the model. The reverse pattern is predicted for environmental expansion. No systematic path integration errors should be expected if the outbound displacement and return vectors are both computed from only the original or only the rescaled grid periods.

We capitalized on the rescaling property of grid cells [10] to test this neurally based model of the function of grid cells in human path integration. Participants followed an unpredictable five-segment outbound path in immersive virtual reality and then attempted to walk directly back to the first waypoint without vision (Figure 2; [15]). Each experimental block consisted of three "priming" trials, in which the enclosure's shape was constant, and one "deformation" trial, in which the enclosure expanded or contracted symmetrically along one dimension (Figure S1). We assumed that the priming trials would enable the formation of a stable grid cell map, which in the deformation trial was hypothesized to expand or contract according to the corresponding change in enclosure shape. The shortest return path from the final waypoint to the first waypoint in the deformation trial was parallel to the changed dimension (changed condition) or to the unchanged dimension (unchanged condition) of the enclosure. Matched return paths in priming trials were of the same length and orientation as those in the deformation trials and served as supplementary measures of baseline performance. Outbound displacements and return paths in the matched, changed, and unchanged conditions were identical. Random return paths in priming trials were not controlled and varied in length and orientation from those in matched priming trials and deformation trials.

In experiments 1A and 1B, the enclosure was square in the priming trials and expanded or contracted along one axis to be rectangular in the deformation trial. Participants walked shorter

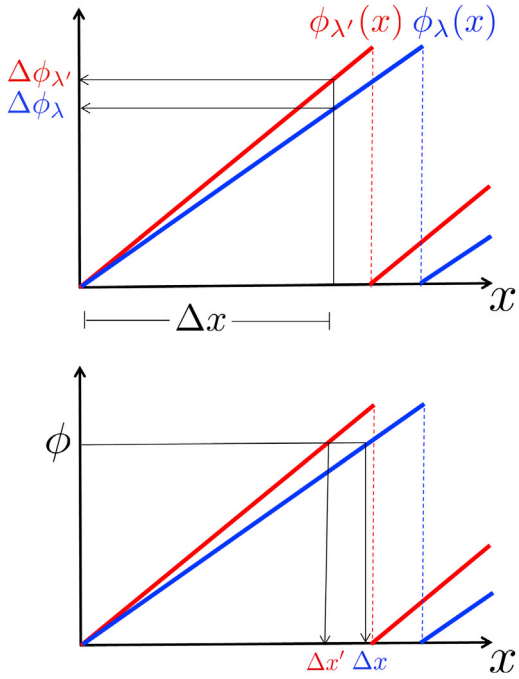

Figure 1. One-Dimensional Schematic Illustration of the Grid Cell Phase Code for Space

The figure shows a single spatial period (λ; blue) and a rescaled version ($\lambda' < \lambda$; red) in response to the shrinking of an enclosure dimension. Top: a displacement Δx corresponds to a larger phase change in the compressed than the uncompressed grid response. Bottom: a phase ϕ corresponds to a larger displacement when decoded with respect to the uncompressed grid response. Alternatively, if ϕ results from an encoding using the uncompressed grid response and is decoded using the compressed grid response (as in experiment 3B), a smaller displacement is recovered. See Supplemental Information for the proof of the general case.

distances when returning parallel to the stretched than the unstretched axis (Figure 3A) and longer distances when returning parallel to the compressed than the uncompressed axis (Figure 3B; mean distance and heading error in Figure 4). In experiments 2A and 2B, the enclosure was rectangular in the priming trials and expanded or contracted to be square in the deformation trial. Participants again walked shorter distances when returning parallel to the stretched than the unstretched axis (Figure 3C) and longer distances when returning parallel to the compressed than the uncompressed axis (Figure 3D). Distances walked on return paths in rectangular priming enclosures were not affected by whether they were parallel to the shorter or the longer axis.

This pattern of homing errors should reverse if participants encode the outbound displacement using the original grid but compute the return displacement in terms of a deformed grid (Figure 1). In two of three priming trials of experiments 3A and 3B, the landmarks, ground surface, and enclosure were visible during the outbound path, but not the return path, as in previous experiments. In the other priming trial (matched condition; second or third in sequence), the landmarks and the ground surface, but not the enclosure, were visible during the outbound path; the enclosure appeared immediately before the return path was executed. We expected that because distal landmarks remained the same and the familiar enclosure was present on the return path, participants would view the environment as familiar and the grid network would remain unchanged in this priming trial [16]. The deformation trial was the same as this priming trial except that the enclosure was expanded or contracted along one axis relative to the three priming trials. Our conjecture was that in the deformation trial, the location of the first waypoint would be represented in terms of phases of the original grid during the outbound path but those phases would be decoded using the deformed grid during the return path, with the prediction that participants should now undershoot the target along the contracted dimension and overshoot it when that dimension is expanded. As shown in Figures 3E and 3F, this pattern of results was obtained. Results of experiments 1–3 did not seem to be under top-down cognitive control (see Supplemental Information).

Barry et al. [10] observed that when one dimension of the environment was expanded or contracted, there was a corresponding rescaling of the grid network along that dimension and a small but significant rescaling of opposite sign for the perpendicular dimension. This effect was present in the results of experiments 1–3 (Figure 4A). The difference between changed and matched (baseline) conditions was in the opposite direction as the difference between unchanged and matched conditions. This reversed bias for the unchanged condition (experiment 1A, matched − unchanged; experiment 1B, unchanged − matched; etc.) averaged −.057 m across participants, $t(71) = -2.105$, $p = 0.039$. By comparison, bias for the changed condition averaged 0.196 m, $t(71) = 5.822$, $p = 0.000$ (experiment 1A, matched − changed; etc.). This is the pattern of bias expected if grid networks rescale in opposite directions along the changed and the unchanged dimensions of the deformed enclosure.

DISCUSSION

Our findings do not show that grid cells exist in humans. The contributions of the present project are to show, first, that a mathematical model of location coding by grid cells can be combined with empirical findings on rescaling of grid cells in rats to generate novel predictions of bias in human path integration in response to changes in environmental geometry and, second, that those behavioral predictions are confirmed experimentally. We are not aware of other models of path integration that predict these findings a priori [12, 17–22].

Two closely related projects are O'Keefe and Burgess (OB; [23]) and Hartley, Trinkler, and Burgess (HTB; [24]). OB examined deformations of place fields in rats in response to expansions and contractions of rectilinear enclosures. Properties of place fields were broadly consistent with bias along the changed dimension in experiments 3A and 3B. OB's empirical findings and place-field models do not seem to predict reversed bias perpendicular to the changed dimension.

HTB investigated in humans the effects of enclosure deformation on memory of a target's location using visual cues alone. They attempted to minimize the use of path integration by testing participants in desktop virtual reality (in which idiothetic self-motion cues are not available) and by partially disorienting participants prior to testing. Participants tended to place targets

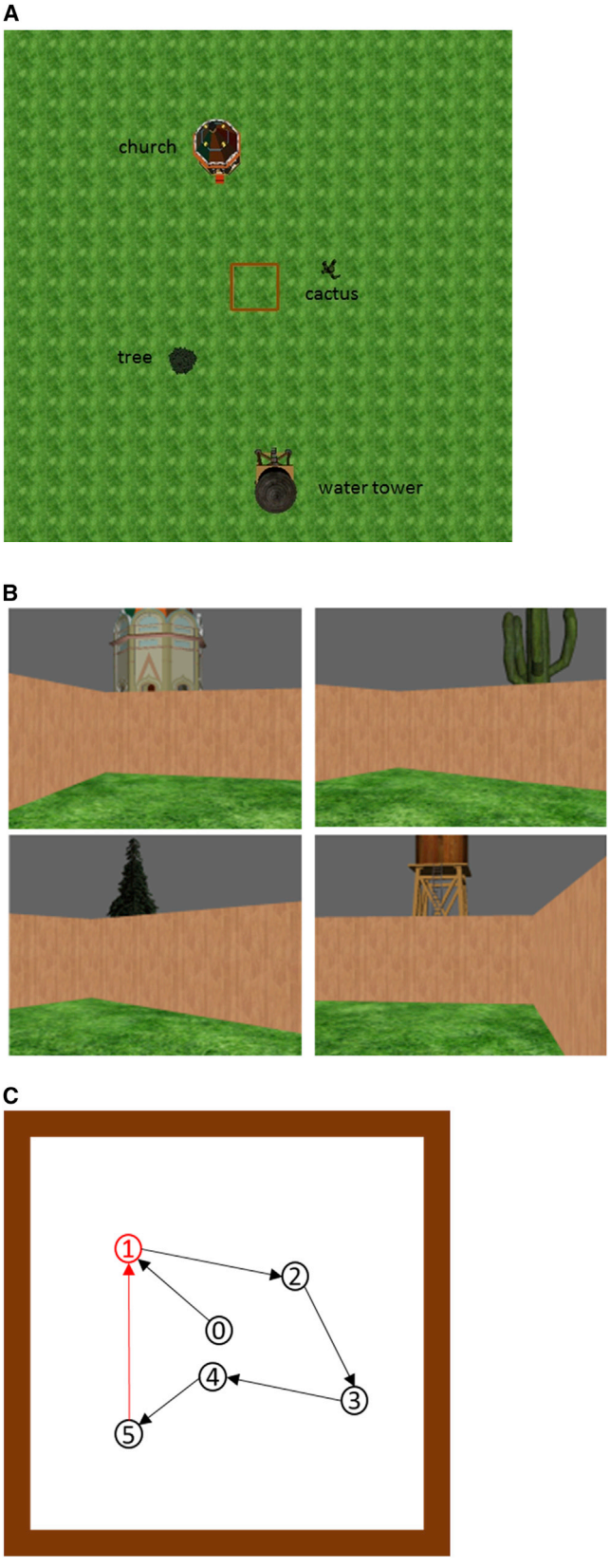

Figure 2. Apparatus and Sample Path

Virtual environments were displayed stereoscopically in the head-mounted display (HMD) worn by participants. The immersive technology converted walking and turning in the real world into corresponding motion in the virtual world, allowing participants to experience natural vestibular and proprioceptive motion cues. Gains between visual and body-based information were always matched (cf. [13, 14]).

(A) Participants locomoted within a virtual enclosure (brown square). Four landmarks were visible over the enclosure walls to provide orientation cues.

(B) Screen shots from the HMD.

(C) Example of a path. Black arrows constitute outbound path; red arrow represents return path. Each trial began with participant standing at location 0 in the center of the enclosure.

at fixed distances or fixed ratios of distances to enclosure boundaries. This effect is consistent with bias along the changed dimension in experiments 3A and 3B. HTB also observed a small bias in the opposite direction perpendicular to the changed dimension. They suggested that such an effect was consistent with a representation of location based on angles to the four corners of the enclosure, although this model fit their data less well overall and did not account for a key interaction between target position and type of deformation.

Is it possible that HTB's findings were influenced by the engagement of the grid-cell-based path integration system? Previous studies have detected grid cell-like activity in humans using desktop virtual reality [8, 9], suggesting that the grid cell system may be engaged by path integration based on optical flow in the absence of body-based cues. The natural navigation conditions used in our experiments would have enhanced the involvement of the grid cell system and reliance on path integration and may account for the fact that the reversed bias perpendicular to the changed dimension was much larger in magnitude than in HTB's experiment. Experiments 3A and 3B were similar to HTB's in terms of the availability of visual cues during target localization and also produced the smallest reversed bias effect of our experiments.

Patterns of bias similar to those observed here could occur if the participant's perception of speed were affected by deformations of the enclosure (e.g., if locomotion parallel to an expanded dimension of the enclosure leads to the perception of slower speed and hence smaller perceived displacement on the outbound path). Distorted speed perception for motion parallel to the changed dimension cannot, by itself, account for the reversed bias in the unchanged condition. To explain the reversed bias, one must additionally assume that speed perception for motion perpendicular to the changed dimension is altered in the opposite way as for motion parallel to the changed dimension (perhaps through normalization or regression to the mean of estimated speed across all directions of motion). Analyses of physical walking speed did not produce evidence that the behavioral biases in path integration were produced by distorted speed perception (Supplemental Information).

It is possible that rescaling in speed perception is responsible for both grid distortion [10] and biases in our tasks. This conjecture is purely hypothetical and remains to be tested. Our model of location coding by grid cells combined with the empirical findings of Barry et al. predict the bias and reversed bias effects a priori, regardless of the ultimate mechanism of grid distortion.

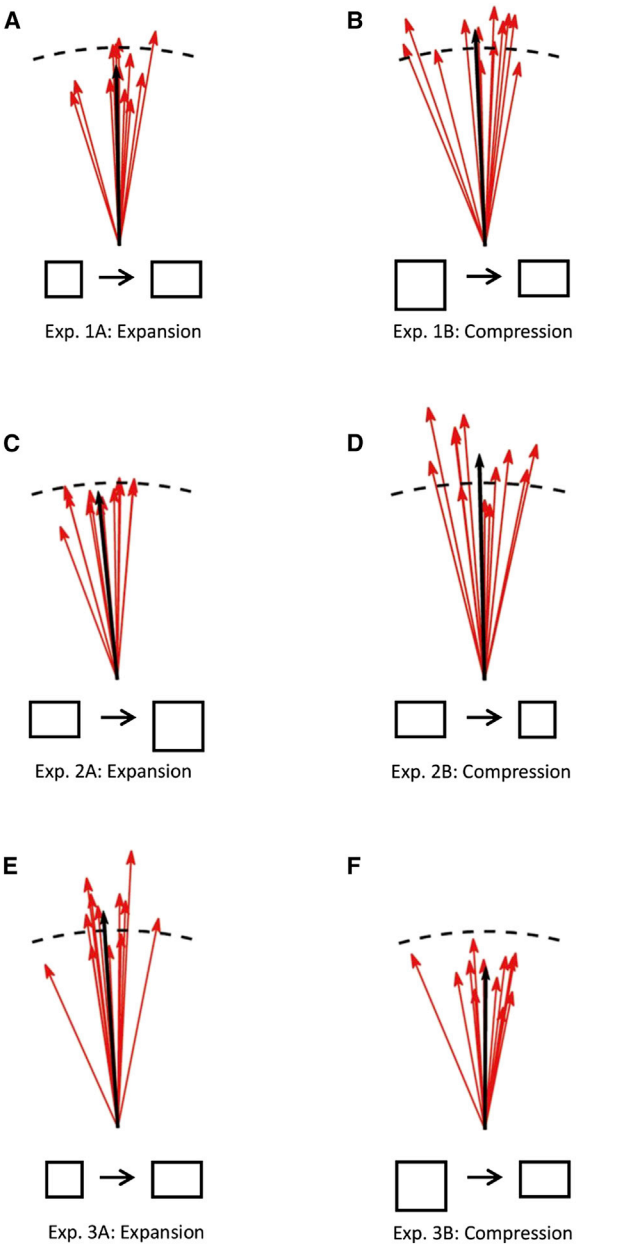

(In panels **E** and **F** the enclosure was not visible on the outbound path but was visible on the return path in one priming trial and the deformation trial)

Figure 3. Normalized Path Integration Performance in Experiments 1–3

Each red vector represents the normalized mean performance of one participant. The length of each vector corresponds to the ratio of the mean walked distance on the return path in the changed condition relative to the unchanged condition, and its orientation corresponds to the mean signed heading error across changed and unchanged conditions. Correct return paths are rotated to a common heading of 0°. Vector mean is in black. Dashed arc represents equivalent performance in the changed and the unchanged conditions.

(A and B) Experiments 1A and 1B, square to rectangular.

(C and D) Experiments 2A and 2B, rectangular to square.

(E and F) Experiments 3A and 3B, square to rectangular (in experiments 3A and 3B, the enclosure was not visible during the outbound path but was visible during the return path in one priming trial and the deformation trial).

Our model assumes that all grids whose phases are used in the location code rescale by the same amount. The modular organization of grid cells in rat [10, 25] suggests that location information from independent scale-orientation modules may be pooled to construct a representation of location. If environmental deformation affects some modules but not others, as suggested by the findings of Stensola et al., an integrative process of location retrieval could explain why average proportional bias in the present experiments was less than the magnitude of environmental deformation. It is noteworthy that the proportional bias averaged 31% of the magnitude of environmental deformation in our experiments and the degree of module rescaling averaged 35% in Stensola's experiments ($t(71) = 0.835$, $p = 0.407$).

Grid cell firing patterns are regular and coherent, which facilitates observing and measuring distortions produced in those patterns by geometric manipulations of the environment. The biases seen in human path integration from similar manipulations match the distortions seen in grid firing patterns. However, they are also similar to less well-characterized changes seen in place cell firing. It is likely that biases in behavior reflect distortions present throughout the brain networks responsible for tracking self-location and generating spatial responses. Our participants reported using various cognitive strategies to locate the target (e.g., attending to distal landmarks, using boundaries as landmarks) and must have experienced using memories of the environments to guide their return paths [26–28]. Our conjecture in experiments 1 and 2 that grid spacing was restored when participants executed the return path might correspond at the cognitive level to using memories of the priming enclosure to guide the return path; likewise, the assumption in experiment 3 that grid spacing was maintained during the outbound path in distortion trials might correspond at the cognitive level to imagining the priming enclosure during the outbound path (see Supplemental Information for tests of one such model). Understanding the relationships between cognitive representations and neural processing in grid, place, and other spatially selective cells is a key domain of future research in human spatial memory and navigation.

EXPERIMENTAL PROCEDURES

Participants

Each experiment had 12 participants (gender balanced) with normal or corrected-to-normal vision. All procedures were approved by the Vanderbilt University Institutional Review Board.

Stimuli and Design

Possible post locations were arranged in circular arrays as shown in Figure S2. The entire array was never visible during an experiment. Each experiment consisted of 16 blocks of 3 priming trials and 1 deformation trial (Figure S1). Enclosures expanded from 5 × 5 m to 5 × 7 m (experiments 1A and 3A), contracted from 7 × 7 m to 5 × 7 m (experiments 1B and 3B), expanded from 5 × 7 m to 7 × 7 m (experiment 2A), or contracted from 5 × 7 m to

Directional t tests showed that the mean vector length differed significantly from 1 in all experiments. Degrees of freedom [df] = 11; (A): $\overline{v} = 0.913$, $t = -2.57$, $p = 0.013$; (B): $\overline{v} = 1.096$, $t = 3.57$, $p = 0.002$; (C): $\overline{v} = 0.962$, $t = -1.90$, $p = 0.042$; (D): $\overline{v} = 1.148$, $t = 2.93$, $p = 0.007$; (E): $\overline{v} = 1.101$, $t = 2.25$, $p = 0.023$; (F): $\overline{v} = 0.833$, $t = -5.76$, $p < 0.001$. Mean signed heading error differed from 0 only in (C): $\overline{\theta} = -4.551°$, $t = 2.41$, $p = 0.034$ (two-tailed); all other $|t| \leq 1.8$.

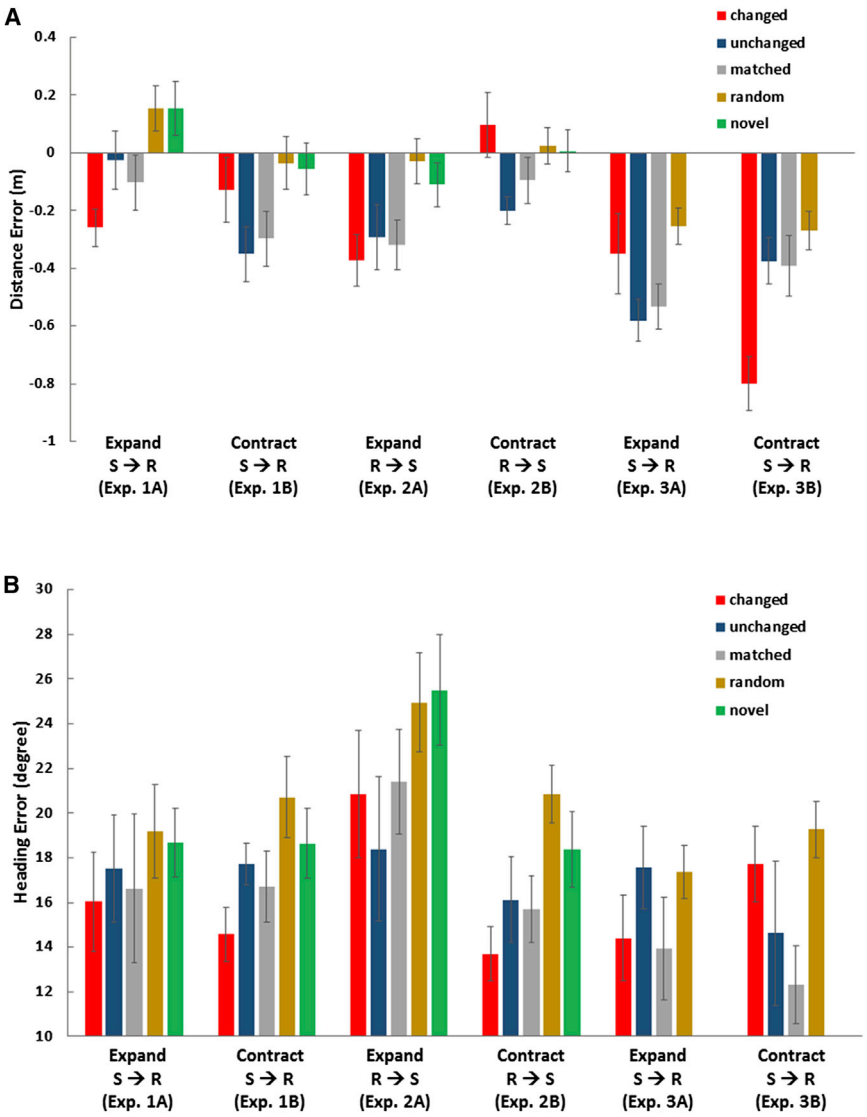

Figure 4. Distance and Heading Error on Return Paths in Priming and Deformation Trials in Experiments 1–3

Enclosure expanded or contracted from square (S) to rectangular (R) or vice versa between prime trials and deformation trial. Conditions defined in text. Error bars show ±SE.

(A) Distance error (walked distance − correct distance). In each conceptual pair of experiments, the interaction between expansion-contraction and changed-unchanged was statistically reliable. Experiments 1A and 1B: $F(1,22) = 17.597$, $p < 0.001$; experiments 2A and 2B: $F(1,22) = 14.521$, $p = 0.001$; experiments 3A and 3B: $F(1,22) = 25.426$, $p < 0.001$. Holm-Bonferroni comparisons of changed, unchanged, and matched conditions yielded the following for changed versus unchanged: experiment 1A, $\alpha = 0.017_{(F\alpha = 0.05)} < p = 0.019 < \alpha = 0.033_{(F\alpha = 0.10)}$; experiment 1B, $p = 0.007 < \alpha = 0.017_{(F\alpha = 0.05)}$; experiment 2A, $p = 0.054 > \alpha = 0.033_{(F\alpha = 0.10)}$; experiment 2B, $p = 0.008 < \alpha = 0.017_{(F\alpha = 0.05)}$; experiment 3A, $p = 0.042 > \alpha = 0.033_{(F\alpha = 0.10)}$; experiment 3B, $p < .001 < \alpha = 0.017_{(F\alpha = 0.05)}$. The unchanged and matched conditions did not differ significantly in any of the experiments (all $p > 0.07$).

(B) Absolute heading error (|walked heading − correct heading|). The changed and unchanged conditions differed significantly only in experiment 1B: $p = 0.004 < \alpha = 0.017_{(F\alpha = 0.05)}$ (all other $p > 0.3$). Considering that differences in heading error might have affected results on distance error, we calculated the corrected distance error, which represents distance disparity along the direction of the correct return path (= walked distance × cos(absolute heading error) − correct distance); results were similar to original variable.

5 × 5 m (experiment 2B). The changed dimension was counterbalanced in each experiment.

Procedure

Participants started each trial standing at the enclosure center and facing a designated direction of 0° (indicated by markers and constant for the experiment). The environment then appeared. One of the posts appeared in red, and participants walked to it. Once they arrived, the red post disappeared, and a green post appeared (blue in experiments 3A and 3B). Participants were shown and walked to four green (or blue) posts successively, with each post disappearing when the participant arrived. To execute the return path, participants walked from the final post to the remembered location of the first red post. Dependent measures were the distance and the direction walked by participants on the return path. No feedback was provided. Prior to the experiment, participants received eight practice trials in the familiar priming environment. The experiment lasted about 2 hr per participant.

Data Analysis

Approximately 1% of data were lost due to technical problems. Trials with heading error greater than 90° were eliminated (3.3% of all trials).

SUPPLEMENTAL INFORMATION

Supplemental Information includes Supplemental Experimental Procedures and four figures and can be found with this article online at http://dx.doi.org/10.1016/j.cub.2015.05.031.

AUTHOR CONTRIBUTIONS

T.P.M., X.C., and J.W.K. designed the experiments. X.C. and Q.H. conducted the experiments, analyzed data, and prepared most of the figures. I.R.F. provided the proof in the Supplemental Information. X.C. and T.P.M. wrote the first draft of the paper. All authors contributed to the final version of the paper.

ACKNOWLEDGMENTS

We thank Neil Burgess, Randolph Blake, Barton L. Anderson, Isabel Gauthier, and three reviewers for comments. This work was supported by grants from the National Science Foundation (HCC 0705863, MRI 0821640; R. Bodenheimer, principal investigator [PI]; T.P.M., Co-PI) and grants to I.R.F. from the McKnight Scholar Award Program, National Science Foundation (EAGER 1148973), and Office of Naval Research Young Investigator Program (N000141310529).

Received: April 23, 2014
Revised: April 1, 2015
Accepted: May 14, 2015
Published: June 11, 2015

REFERENCES

1. Gallistel, C.R. (1990). The Organization of Learning. (Cambridge: MIT Press).
2. Mittelstaedt, M.L., and Mittelstaedt, H. (1980). Homing by path integration in a mammal. Naturwissenschaften *67*, 566–567.
3. Boccara, C.N., Sargolini, F., Thoresen, V.H., Solstad, T., Witter, M.P., Moser, E.I., and Moser, M.-B. (2010). Grid cells in pre- and parasubiculum. Nat. Neurosci. *13*, 987–994.
4. Hafting, T., Fyhn, M., Molden, S., Moser, M.-B., and Moser, E.I. (2005). Microstructure of a spatial map in the entorhinal cortex. Nature *436*, 801–806.
5. Fyhn, M., Hafting, T., Treves, A., Moser, M.-B., and Moser, E.I. (2007). Hippocampal remapping and grid realignment in entorhinal cortex. Nature *446*, 190–194.
6. Killian, N.J., Jutras, M.J., and Buffalo, E.A. (2012). A map of visual space in the primate entorhinal cortex. Nature *491*, 761–764.
7. Yartsev, M.M., Witter, M.P., and Ulanovsky, N. (2011). Grid cells without theta oscillations in the entorhinal cortex of bats. Nature *479*, 103–107.
8. Jacobs, J., Weidemann, C.T., Miller, J.F., Solway, A., Burke, J.F., Wei, X.-X., Suthana, N., Sperling, M.R., Sharan, A.D., Fried, I., and Kahana, M.J. (2013). Direct recordings of grid-like neuronal activity in human spatial navigation. Nat. Neurosci. *16*, 1188–1190.
9. Doeller, C.F., Barry, C., and Burgess, N. (2010). Evidence for grid cells in a human memory network. Nature *463*, 657–661.
10. Barry, C., Hayman, R., Burgess, N., and Jeffery, K.J. (2007). Experience-dependent rescaling of entorhinal grids. Nat. Neurosci. *10*, 682–684.
11. Fiete, I.R., Burak, Y., and Brookings, T. (2008). What grid cells convey about rat location. J. Neurosci. *28*, 6858–6871.
12. Sheynikhovich, D., Chavarriaga, R., Strösslin, T., Arleo, A., and Gerstner, W. (2009). Is there a geometric module for spatial orientation? Insights from a rodent navigation model. Psychol. Rev. *116*, 540–566.
13. Rieser, J.J., Pick, H.L.J., Jr., Ashmead, D.H., and Garing, A.E. (1995). Calibration of human locomotion and models of perceptual-motor organization. J. Exp. Psychol. Hum. Percept. Perform. *21*, 480–497.
14. Tcheang, L., Bülthoff, H.H., and Burgess, N. (2011). Visual influence on path integration in darkness indicates a multimodal representation of large-scale space. Proc. Natl. Acad. Sci. USA *108*, 1152–1157.
15. Kelly, J.W., McNamara, T.P., Bodenheimer, B., Carr, T.H., and Rieser, J.J. (2008). The shape of human navigation: how environmental geometry is used in maintenance of spatial orientation. Cognition *109*, 281–286.
16. Barry, C., Ginzberg, L.L., O'Keefe, J., and Burgess, N. (2012). Grid cell firing patterns signal environmental novelty by expansion. Proc. Natl. Acad. Sci. USA *109*, 17687–17692.
17. Burgess, N., Barry, C., and O'Keefe, J. (2007). An oscillatory interference model of grid cell firing. Hippocampus *17*, 801–812.
18. Byrne, P., Becker, S., and Burgess, N. (2007). Remembering the past and imagining the future: a neural model of spatial memory and imagery. Psychol. Rev. *114*, 340–375.
19. Hasselmo, M.E., Brandon, M.P., Yoshida, M., Giocomo, L.M., Heys, J.G., Fransen, E., Newman, E.L., and Zilli, E.A. (2009). A phase code for memory could arise from circuit mechanisms in entorhinal cortex. Neural Netw. *22*, 1129–1138.
20. Fuhs, M.C., and Touretzky, D.S. (2006). A spin glass model of path integration in rat medial entorhinal cortex. J. Neurosci. *26*, 4266–4276.
21. McNaughton, B.L., Battaglia, F.P., Jensen, O., Moser, E.I., and Moser, M.-B. (2006). Path integration and the neural basis of the 'cognitive map'. Nat. Rev. Neurosci. *7*, 663–678.
22. Fujita, N., Klatzky, R.L., Loomis, J.M., and Golledge, R.G. (1993). The encoding-error model of path competion without vision. Geogr. Anal. *25*, 295–314.
23. O'Keefe, J., and Burgess, N. (1996). Geometric determinants of the place fields of hippocampal neurons. Nature *381*, 425–428.
24. Hartley, T., Trinkler, I., and Burgess, N. (2004). Geometric determinants of human spatial memory. Cognition *94*, 39–75.
25. Stensola, H., Stensola, T., Solstad, T., Frøland, K., Moser, M.-B., and Moser, E.I. (2012). The entorhinal grid map is discretized. Nature *492*, 72–78.
26. Kalia, A.A., Schrater, P.R., and Legge, G.E. (2013). Combining path integration and remembered landmarks when navigating without vision. PLoS ONE *8*, e72170.
27. Philbeck, J.W., Klatzky, R.L., Behrmann, M., Loomis, J.M., and Goodridge, J. (2001). Active control of locomotion facilitates nonvisual navigation. J. Exp. Psychol. Hum. Percept. Perform. *27*, 141–153.
28. Philbeck, J.W., and O'Leary, S. (2005). Remembered landmarks enhance the precision of path integration. Psicologica (Valencia) *26*, 7–24.

